Vessel Segmentation Using A Shape Driven Flow

Delphine Nain, Anthony Yezzi and Greg Turk
Georgia Institute of Technology, Atlanta GA 30332, USA
{delfin, turk}@cc.gatech.edu, ayezzi@ece.gatech.edu

Abstract. We present a segmentation method for vessels using an implicit deformable model with a soft shape prior. Blood vessels are challenging structures to segment due to their branching and thinning geometry as well as the decrease in image contrast from the root of the vessel to its thin branches. Using image intensity alone to deform a model for the task of segmentation often results in leakages at areas where the image information is ambiguous. To address this problem, we combine image statistics and shape information to derive a region-based active contour that segments tubular structures and penalizes leakages. We present results on synthetic and real 2D and 3D datasets.

1 Introduction

Blood vessel segmentation and visualization of blood vessels is important for clinical tasks such as diagnosis of vascular diseases, surgery planning and blood flow simulation. A number of methods have been developed for vessel segmentation, however most of those techniques do not use a shape prior, or use a strong shape prior. With strong shape priors, such as shape templates, the segmentation is constrained to a particular shape space. Since diseased vessels can have abnormal shapes, a strict shape template may result in incorrect segmentation that misses important anatomical information. However, using image intensity alone for the task of segmentation often results in leakages perpendicular to the vessel walls at areas where the image information is ambiguous. Leakages cause the segmented model to expand into areas that are not part of the vessel structure, and results in incorrect segmentation. In this paper, we introduce the notion of segmentation with a *soft* shape prior, where the segmented model is not constrained to a predefined shape space, but is penalized if it deviates strongly from a tubular structure, since those deviations have a high probability of being leaks. Our method uses a soft shape prior in addition to image statistics to deform an active contour for the task of blood vessel segmentation.

2 Related Work

Many geometric methods exist for vessel segmentation that range from using no shape priors to strong shape priors. Tubular structures can be identified by the response of derivative and Gaussian filters convolved with the image. Sato et al. use the second derivatives of a set of multiscale gaussian filters to detect curvilinear structures and penalize high intensity (bumps) on the vessel walls [1]. The filter response can be used to visualize the vessels through Maximum Intensity Projections (MIP) or isosurface extraction. Since these methods rely on the intensity of the image, a noisy intensity map may result in incorrect filter response and additional shape information might be needed for a correct

segmentation. Skeletons [2, 3] can be used as a basis of graph analysis of vessels, and further processing is needed to extract the 3D shape of the vessel. Krissian et al. use multiscale filtering, based on a set of gaussian kernels and their derivatives to extract a skeleton of vasculature [5]. The local maxima of the filter response is used to find centerpoints and radius information in order to fit a cylindrical model to the data. The restriction of the shapes can be a limitation since diseased vessels can have cross-section that deviate from an elliptical shape.

Deformable models are a powerful technique for flexible automatic 3D segmentation. Deformable models are based on an initial contour or surface deformed by a combination of internal (shape) and external (image and user defined) forces to segment the object of interest. In particular, the addition of a shape prior as an internal force can greatly increase the robustness of deformable models when applied to the task of vessel segmentation. Snakes are parametrized models and shape templates can easily be incorporated in this framework [6, 9]. However those methods have a limitation since the surface cannot handle topological changes as easily as the level set methods and reparameterization is often necessary and complex in 3D. Level set methods represent a surface implicitly by the zero level set of a scalar-valued function. The evolution is carried out within this framework without the need for parameterization or explicit handling of topological changes [7, 8]. However, since there is no explicit parameterization, incorporating a shape prior in this framework is more difficult.

To address the issue of leaks that form at the root of vessels during a fast marching segmentation, Deschamps et al. [4] freeze a percentage of the points that are closer to the starting seed (since it is assumed that they have segmented the structure of interest) while allowing the fast evolving points to evolve normally. This technique does not prevent leaks that form far away from the root of the vessels, close to the fast evolving part of the front.

Leventon et al. [10] use dimensionality reduction techniques on the distance transform of a set of previously segmented shapes to define a shape constraint within a level set framework. This technique yields good results, but requires pre-segmented data. It has also not been tested on vessel structures. Strong shape priors in combination with level set techniques for vessel segmentation was used by Lorigo et al. [11]. They evolve 1D curves in a 3D volume and then estimate the radius of the vessels locally using the inverse of principal curvature. The advantage of this technique is that it does not require pre-segmented data, however it makes a strong assumption about the shape of the vessels since they are modeled as tubes with varying width. To our knowledge, no existing level set techniques use a soft shape prior for vessel segmentation.

3 Shape Driven Flow

3.1 Region Based Flow

Our base flow deforms the curve of interest according to a smoothing term and an image term ϕ. In this paper, we use an adaptive threshold with decaying intensity from the root of the vessel (determined by the seed point of the initial contour) to the rest of the contour.

We define the following energy in the region R inside the curve C parameterized by arc-length s:

$$E(C) = -\int_R \phi d\mathbf{x} + \int_C ds \qquad (1)$$
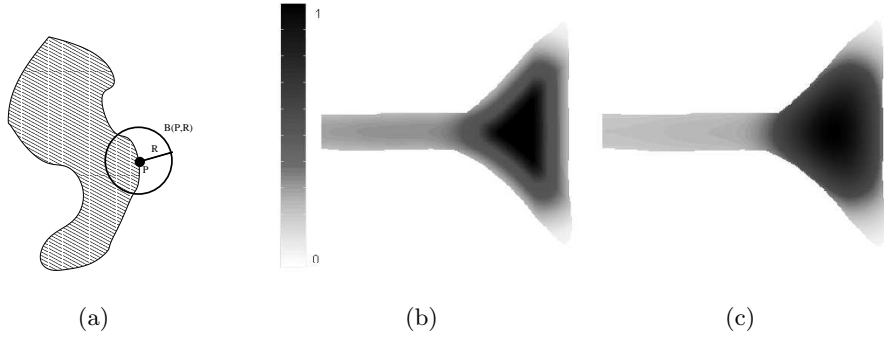
(a)   (b)   (c)

Fig. 1. (a) $\epsilon_1(\mathbf{x})$ is the intersection of the ball centered at $\mathbf{x}$ and the region R inside the contour. (b) Points inside the widening region have a higher ϵ_1 measure but most points on the contour have the same measure. (c)Contour points close to the widening of the contour have a higher ϵ_2 measure

This is a region based active contour. We minimize Equation 1 by computing its first variation and solving the obtained Euler-Lagrange equation by means of gradient descent. We find the following curve evolution equation:

$$\frac{\partial C(\mathbf{x})}{dt} = (-\phi(\mathbf{x}) + \kappa(\mathbf{x}))\mathcal{N} \qquad (2)$$

where ϕ is a speed determined by the underlying image, $\kappa(x)$ is the curvature of the curve at point x and $\mathcal{N}$ is the unit inward normal to the curve. We evolve this active contour using Level Set Techniques[7, 8].

Image statistics alone might lead to unsatisfactory segmentations. Figure 5(a) shows an example of very noisy image data where areas of pixels close to the vessel have very similar image statistics. This results in a leak when segmented with the type of flow (2). More sophisticated algorithms can be devised based on image statistics or prior knowledge such as multiscale filter responses tuned to detect vessels [13, 6, 14], but these algorithms will be very specific to the type of data and image acquisition. This leakage problem can be addressed in a more general way by adding a soft shape constraint to the flow so that the algorithm penalizes obvious leaks.

3.2 Shape Filters

We would like to locally determine the shape of a contour, and particularly areas where it is widening and potentially leaking. The information from derivatives of the curve, such as curvature, is too local since widening of the contour cannot be discriminated from small noise and bumps. We propose to use a local filter at a scale larger than the derivative scale. We define a local neighborhood $B(\mathbf{x}, r)$ in the shape of a ball (disk in R^2, solid sphere in R^3) centered at the point $\mathbf{x}$ and of radius r, see Figure 1(a). For every point $\mathbf{x}$ inside and on the contour (region R), we define a filtering operation that calculates a measure ϵ_1 in the neighborhood $B(\mathbf{x}, r)$. The measure ϵ_1 is the percentage of points that fall both within the ball centered at $\mathbf{x}$ and the region R inside the contour[1]:

$$\epsilon_1(\mathbf{x}) = \int_{B(\mathbf{x},r)} \mathcal{X}(\mathbf{y})d\mathbf{y} \quad \text{where } \mathcal{X}(\mathbf{y}) = \begin{cases} 1 \; if \; \mathbf{y} \in R \\ 0 \; if \; \mathbf{y} \notin R \end{cases} \qquad (3)$$

---

[1] If $R \to 0$, then $\epsilon_1(\mathbf{x})$ is just the curvature at $\mathbf{x}$.

The parameter r must be chosen by the user and be an upper bound to the expected radius of the vessels. In our simulations, the user picked the width of the largest vessel with the mouse to define r.

The filter response ϵ_1 for a synthetic shape that represents a potential leak is shown in Figure 1(b). Given a radius that is the width of the tube, the points inside the widening region will have a higher measure than the points inside the tube. We will formalize this observation in the next Section by defining an energy minimization that uses the measure ϵ_1 to penalize regions inside the contour that deviate from a tubular shape.

3.3 Curve Evolution using Local Filters

We define such an energy as:

$$E(C) = -\int_R \phi d\mathbf{x} + \int_C ds + \alpha \int_R \epsilon_1^p(\mathbf{x}) d\mathbf{x} \qquad (4)$$

The first and second term are the same as for the region flow previously introduced. The third term is a constraint on shape. When we minimize $E(C)$, the third term will force deviations from tubular shapes to be penalized. In order to obtain a curve evolution formula, we take the first variation of Equation 4. The first variation for such an equation with nested integrals was derived in [12] and we give its solution:

$$\frac{\partial C(\mathbf{x})}{\partial t} = \left(-\phi(\mathbf{x}) + \kappa + \alpha \epsilon_2(\mathbf{x}, p)) \right) \mathcal{N} \qquad (5)$$

where

$$\epsilon_2(\mathbf{x}, p) = \epsilon_1^p(\mathbf{x}) + p \int_{B(\mathbf{x}, r)} \epsilon_1^{p-1}(\mathbf{y}) \mathcal{X}(\mathbf{y}) d\mathbf{y} \qquad (6)$$

The measure ϵ_2 is again the output of a local ball filter. For a point, the response is its ϵ_1 measure plus the sum of the ϵ_1 measure of its neighbouring points that are inside the contour. For a radius r similar to the vessel width, most points on the contour have the same ϵ_1 measure since locally the same percentage of neighbors fall within the filter radius. This can be seen in Figure 1(b), on the left. To see if the contour point lies near a leak region, it is necessary to look at the ϵ_1 measure of its neighbors *inside* the contour since their measure is high for points inside widening regions. This is what ϵ_2 measures, as shown in Figure 1(c), on the right. We observe that contour points close to the widening of the contour have a higher measure than contour points on the tube [2].

Since ϵ_2 is always positive, the third part of Equation 5 is an erosion term (flow along the inward normal) that is proportional to the ϵ_2 measure. At a point with a high measure, the contour shape deviates from a tubular shape and therefore the flow is penalized. The parameter α is chosen according to the amount of penalty desired.

The filter operations are computationally expensive since at every time step, ϵ_1 is calculated for every point inside the curve and ϵ_2 is calculated for every point on the contour. As an optimization, we only recompute the filter outputs for the contour points that have moved since the previous time step and propagate the information to the neighbors that fall within the filter radius.

---

[2] In our implementation, we scale both measure to lie between 0 and 1 so that all three terms in Equation 6 have similar scaling.
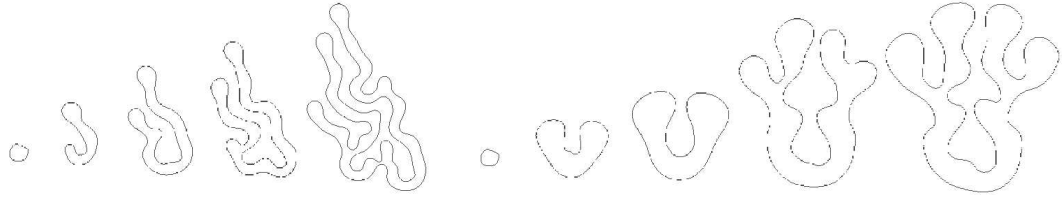
(a) Evolution in time, *p*=2, *r*=20, α=0.75

(b) Evolution in time, *p*=2, *r*=40, α=0.75

Fig. 2. Dilation Flow with Shape Prior

4 Results

It is interesting to evolve a curve using Equation 5 without an image force, to see the effect that our flow has on the evolution of a small near-circle. We chose $\phi = 1$ (a constant image term) so that without the second and third term of the equation, the curve evolution would be a simple dilation of the circle. We then ran the full curve evolution, with 2 different radii ($r = 20$, $r = 40$, $\alpha = 0.75$). As seen in Figures 2(a) and 2(b), the curve evolves keeping a "tubular" shape at all times. The width of the tube depends on the radius of the local filter.

We now test our flow on both 2D and 3D datasets for synthetic and real data. For all flows presented, the user specified the expected biggest radius by clicking two points on the image. More investigation is needed on the effect of choosing different p, for these results we chose the parameters $p = 2$ because it is well behaved.

4.1 2D Images

In 2D,we first used our flow evolution on a synthetic model of a branching vessel. The radius was chosen to be the largest width of the vessel. We observed that the value of the chosen α influences the penalty on deviations from tubular structures. In Figure 3(a), for $\alpha > 0.65$, we observe an erosion around the branching area since points in that region have a higher measure. Figure 3(b), for $\alpha <= 0.65$, the penalty is softened and the vessel is correctly segmented. This value is used for subsequent segmentations and erosion in branching areas was not observed.

We used our flow on a noisy projection of an angiogram and compared it to the base flow without a shape constraint. We show details of the segmentation where leaks were detected. When the neck of the leak is thin, the leak disconnects from the main vessel as shown in Figure 4. This is because points on the contour
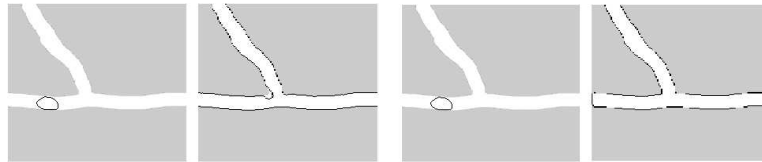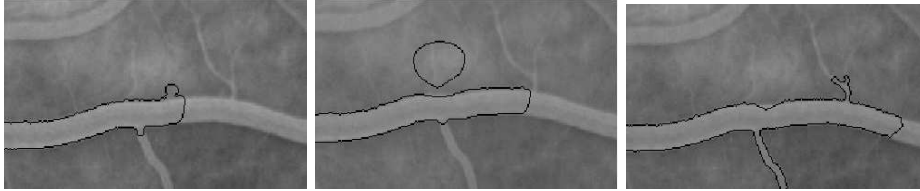

(a) A high penalty α=0.75 causes erosion around the branch.

(b) α=0.65. Erosion around the branch is not observed.

Fig. 3. Flow with Shape Prior on 2D Synthetic Images
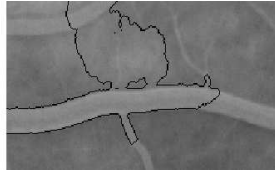
(a) Base Flow, no Shape Prior, 100 iterations

(b) Flow with Shape Prior, at t=50(left), 100(middle) and 200(right) iterations.

Fig. 4. Vessel Flow on Angiogram Images

near the leak region have a high ϵ_2 measure (as can be seen in Figure 1(c)) that causes the contour to erode and eventually pinch off. Once the leak pinches off, the user can then click on the disconnected contour to eliminate it, or the algorithm can detect the change of topology [15] and automatically remove the leakage. The contour points at the neck of the leak are frozen so that the leak does not re-appear while the rest of the contour evolves.

In Figure 5 we observe that the flow with a shape prior is able to prevent many leaks and produce a flow that is much better behaved than the same flow without a shape prior. We notice that without a shape prior, the flow becomes "chaotic" and leaky regions merge with vessel regions (see Figure 5(a)). The repair of such leaks with user interaction would almost amount to a manual segmentation. Figure 5(b), shows that the flow is much better behaved and produces a better segmentation for most of the image. In the left part of the image, we notice an interesting behavior of the shape-constrained flow. This part of the image is very noisy and image statistics are almost identical inside and outside the vessel, so the base flow without a shape prior completely leaks out of the vessel area. The flow with a shape prior also leaks into the background since the image statistics no longer discriminates between foreground and background, but the flow maintains a "vessel-like" shape and the leak is mostly contained. This is important since we do not want the leak to expand to areas of the image that are correctly segmented.
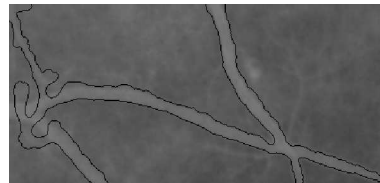
(a) Base Flow, no Shape Prior   (b) Flow with Shape Prior

Fig. 5. Vessel Flow on Angiogram Images

4.2 3D Images

In this section we demonstrate our flow on two 3D CT datasets of a coronary artery. In all Figures, the color on the surface represents the measure ϵ_2. We see that this measure is closely related to the thickness of a vessel.
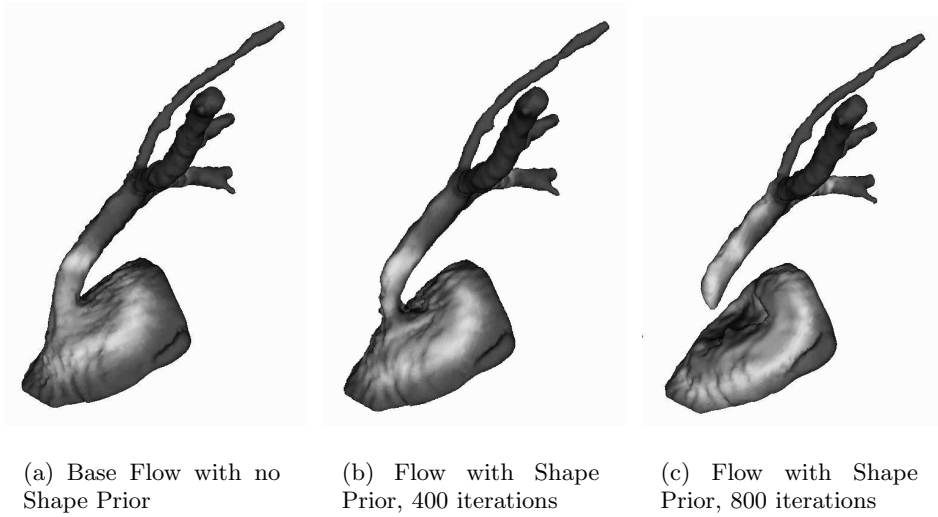
| (a) Base Flow with no Shape Prior | (b) Flow with Shape Prior, 400 iterations | (c) Flow with Shape Prior, 800 iterations |

Fig. 6. Different Flows on the first CT Coronary Data

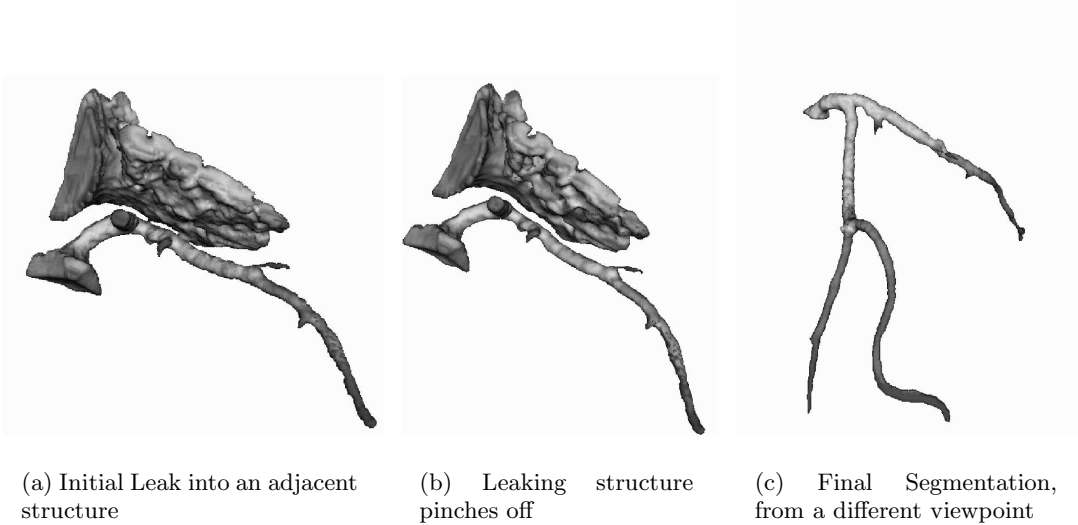| (a) Initial Leak into an adjacent structure | (b) Leaking structure pinches off | (c) Final Segmentation, from a different viewpoint |

Fig. 7. Base Flow with Shape Prior on the second CT coronary dataset

For the first CT coronary dataset, if we use a flow based on image statistics alone, the artery "leaks" into the heart cage (Figure 6(a)). As we can see, the connecting area between the coronary and the heart has the highest measure.

However, when we use the flow with the shape constraint, the leak "pinches" off from the main vessel artery (Figure 6(b) and 6(c)). The second CT coronary dataset leaks into an adjacent structure (Figure 7, left). Again, running the vessel flow separates the coronary from the leak. The user can then click on the isolated leak to remove it. The full segmentation is shown on the right.

5 Conclusion

We have presented a soft shape prior that can be combined with any other image force to deform an active contour and penalize leaks. Although the results presented are still preliminary and need to be medically validated, we found that the shape prior successfully penalizes leak regions and either disconnects the leak from the vessel, or contains the leak. We find these results encouraging since in the presence of noise, the shape driven flow is better behaved than the flow based on image statistics alone. This flow can be combined with minimal user interaction to repair leak effects that were not prevented by the algorithm.

References

1. Y. Sato, S.Nakajima, N. Shiraga, H. Atsumi, S. Yoshida, T. Koller, G. Gerig, and R. Kikinis. Three Dimensional multi-scale line filter for segmentation and visualization of curvilinear structures in medical images. Med.Imag Anal, 1998, 2, 143-168.
2. Flasque N, Desvignes M, Constans JM, Revenu M. Acquisition, segmentation and tracking of the cerebral vascular tree on 3D magnetic resonance angiography images. Med Image Anal. 2001 Sep;5(3):173-83.
3. T. Deschamps, L.D. Cohen. Fast extraction of minimal paths in 3D images and application to virtual endoscopy. Med. Image Anal, 2001 Dec; 5(4).
4. T. Deschamps, L.D. Cohen. Fast Extraction of Tubular and Tree 3D Surfaces with front propagation methods. International Conference on Pattern Recognition, 2002.
5. K. Krissian, G. Malandain, N. Ayache Model-based detection of tubular structures in 3D images. Computer Vision and Image Understanding, 80:2, pp. 130-171,2000.
6. A. Frangi, W. Niessen, K.L. Vincken, and M.A. Viergever Multiscale vessel enhancement filtering. Proc. MICCAI'98, pp.130-137, 1998.
7. S. Osher,R. Fedkiw. Level Set Methods and Dynamic Implicit Surfaces. Springer Verlag, 2002.
8. J.A Sethian. Level Set Methods and Fast Marching Methods. Cambridge University Press, 1999.
9. T. McInerney and D. Terzopoulos. T-snakes:Topology adaptive snakes. Medical Image Analysis,4(2):73-91,2000.
10. M. Leventon, E. Grimson, O. Faugeras. Statistical Shape Influence in Geodesic Active Contours. Comp. Vision and Patt. Recon. (CVPR), June 2000.
11. L. M. Lorigo, O. Faugeras, W. E. L. Grimson, R. Keriven, R. Kikinis, A. Nabavi, C.-F. Westin. Codimension-Two Geodesic Active Contours. Comp. Vision and Patt. Recon. (CVPR), June 2000.
12. G. Aubert, M. Barlaud, O. Faugeras, S. Jehan-Besson. Image Segmentation Using Active Contours: Calculus of Variations or Shape Gradients? SIAM Journal on Applied Mathematics, Volume 63, Number 6, 2003
13. Jr. Yezzi, Anthony, Andy Tsai and Alan Willsky. A Fully Global Approach to Image Segmentation via Coupled Curve Evolution Equations. Journal of Visual Communication and Image Representation, 13 (2002) 195-216.
14. A. Vasilevskiy, K. Siddiqi. Flux-Maximizing Geometric Flows. IEEE Transactions on Pattern Analysis and Machine Intelligence, 24(12), 1565-157 8, 2002.
15. X. Han, C. Xu and J.L Prince. A topology Preserving Level Set Method for Geometric Deformable Models. IEEE Transactions on PAMI, Vol 25, No. 6, pp 755-768, June 2003.